

## Far-from-Equilibrium State in a Weakly Dissipative Model

Eric Bertin<sup>1</sup> and Olivier Dauchot<sup>2</sup>

<sup>1</sup>Université de Lyon, Laboratoire de Physique, Ecole Normale Supérieure de Lyon, CNRS, 46 allée d'Italie, F-69007 Lyon, France

<sup>2</sup>Service de Physique de l'Etat Condensé, CEA Saclay, F-91191 Gif-sur-Yvette Cedex, France

(Received 17 December 2008; published 22 April 2009)

We address, on the example of a simple solvable model, the issue of whether the stationary state of dissipative systems converges to an equilibrium state in the low dissipation limit. We study a driven dissipative zero range process on a tree, in which particles are interpreted as finite amounts of energy exchanged between degrees of freedom. The tree structure mimics the hierarchy of length scales; energy is injected at the top of the tree (large scales), transferred through the tree, and dissipated mostly in the deepest branches of the tree (small scales). Varying a parameter characterizing the transfer dynamics, a transition is observed, in the low dissipation limit, between a quasiequilibrated regime and a far-from-equilibrium one, where the dissipated flux does not vanish.

DOI: 10.1103/PhysRevLett.102.160601

PACS numbers: 05.40.-a, 02.50.Ey, 47.27.eb

One of the main challenges of nonequilibrium statistical physics is to understand which principles rule the description of nonequilibrium steady states. Linear response theory [1] has been developed for systems, subjected to small external gradients, which remain close to equilibrium, and for which the effect of the small drive is thus perturbative. A different situation is that of dissipative systems, in which an energy flux is injected at large scales, and cascades down, through nonlinear interactions, to smaller scales where it is dissipated. Examples include hydrodynamic turbulence [2], wave turbulence in fluids, plasma [3], and vibrating plates [4], fracture [5] and friction [6], granular materials and foams [7]. A natural question is to know whether in the limit of small, but nonzero dissipation, the steady state of the system becomes close to some equilibrium state to be determined. One may expect that adding a tiny amount of injection and dissipation to a conservative system breaks energy conservation, but leads to small fluctuations around a given energy level selected by the injection and dissipation mechanisms. The system would thus merely behave as if it was at equilibrium at this energy.

Whether this scenario holds in general is an open issue. Such approaches have been proposed in the context of two-dimensional turbulence [8], for which the flux of dissipated energy vanishes in the small viscosity limit. However, in other situations such as three-dimensional turbulence [2] or granular gases [9], the dissipated flux remains finite for small viscosity, suggesting that the system does not converge to any equilibrium state.

In order to give further insight into these issues, we study a simple solvable stochastic transport model, namely, an open zero range process (ZRP) [10], that describes in a schematic way the transfer of energy between scales, in the presence of injection and dissipation. To account for the hierarchical organization of scale space, we define our model on a Cayley tree [11], each level being interpreted as a given scale. The advantage of this specific geometry

with respect to more conventional ones (e.g., one-dimensional lattice) is twofold: the tree is self-similar, so that subsystems have the same structure as the global model, and scales are spaced logarithmically, which allows interactions to be treated as local. We show that depending on the energy transfer dynamics, the dissipative stationary state of the model converges in the weak dissipation limit either to an equilibrium state, or to a well-defined far-from-equilibrium state with a finite dissipated flux. The simplicity of our model (nonlinear interactions at play in real systems are replaced by an effective diffusion process) allows us to compute the exact stationary distribution and macroscopic observables of interest. Possible implications of our results for more realistic systems are then discussed.

The model is defined on a Cayley tree composed of  $M$  successive levels (see Fig. 1); at any given level  $j < M$ , all sites have  $m > 1$  forward branches that link them to level  $j + 1$ , so that the number of sites at level  $j$  is  $m^{j-1}$ . Sites are thus labeled by the level index  $j$ , and the index  $i = 1, \dots, m^{j-1}$  within level  $j$ . The energy on each site  $(j, i)$  of the tree is assumed to take only discrete values proportional to an elementary amount  $\varepsilon_0$ , namely  $\varepsilon_{j,i} = n_{j,i}\varepsilon_0$ . Energy transfer proceeds as follows: an energy amount  $\varepsilon_0$  is moved, either forward or backward, along any branch between levels  $j$  and  $j + 1$  with a rate  $v_j$ . In the absence of driving and dissipation, the dynamics satisfies detailed

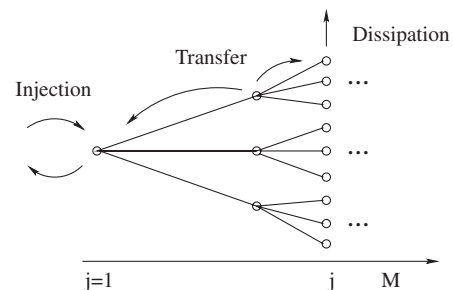


FIG. 1. Sketch of the model, illustrating the tree geometry.

balance. Energy injection is implemented by connecting the site  $(1, 1)$  to a thermostat of temperature  $T_{\text{ext}} = \beta_{\text{ext}}^{-1}$ , with a coupling frequency  $\nu_{\text{ext}}$ . Dissipation proceeds through the random withdrawal of an amount of energy  $\varepsilon_0$  at site  $(j, i)$  with rate  $\Delta_j$ . The master equation governing the evolution of the probability distribution  $P(\{n_{j,i}\}, t)$  reads:

$$\begin{aligned} \frac{\partial P}{\partial t}(\{n_{j,i}\}, t) = & - \left( \sum_{j=1}^{M-1} m^{j-1} (2m\nu_j + \Delta_j) + m^{M-1} \Delta_M + \nu_{\text{ext}} (1 + e^{-\beta_{\text{ext}} \varepsilon_0}) \right) P(\{n_{j,i}\}, t) \\ & + \sum_{j=1}^{M-1} \sum_{i=1}^{m^{j-1}} \sum_{l=1}^m \nu_j [P(n_{j,i} + 1, n_{j+1, (i-1)m+l} - 1, \{n_{q,r}\}, t) + P(n_{j,i} - 1, n_{j+1, (i-1)m+l} + 1, \{n_{q,r}\}, t)] \\ & + \sum_{j=1}^M \sum_{i=1}^{m^{j-1}} \Delta_j P(n_{j,i} + 1, \{n_{q,r}\}, t) + \nu_{\text{ext}} [P(n_{1,1} + 1, \{n_{q,r}\}, t) + e^{-\beta_{\text{ext}} \varepsilon_0} P(n_{1,1} - 1, \{n_{q,r}\}, t)]. \end{aligned} \quad (1)$$

In this last equation,  $\{n_{q,r}\}$  is a shorthand notation for all the variables that are not explicitly listed. Turning to the stationary state, we look for a steady-state probability distribution of the form

$$P_{\text{st}}(\{n_{j,i}\}) = \frac{1}{Z} \prod_{j=1}^M \prod_{i=1}^{m^{j-1}} e^{-\beta_j n_{j,i} \varepsilon_0}, \quad (2)$$

where  $\beta_j$  is an effective inverse temperature (to be determined) associated to level  $j$ , and  $Z$  is a normalization factor. Inserting expression (2) of the stationary distribution into the master equation (1) yields a set of equations to be satisfied by the parameters  $z_j = \exp(-\beta_j \varepsilon_0)$ , for  $j = 2, \dots, M-1$ :

$$\nu_{j-1}(z_{j-1} - z_j) - m\nu_j(z_j - z_{j+1}) = \Delta_j z_j, \quad (3)$$

with the boundary conditions

$$\nu_{\text{ext}}(e^{-\beta_{\text{ext}} \varepsilon_0} - z_1) - m\nu_1(z_1 - z_2) = \Delta_1 z_1, \quad (4)$$

$$\nu_{M-1}(z_{M-1} - z_M) = \Delta_M z_M. \quad (5)$$

Note that these equations correspond to the local balance of the diffusive fluxes  $\nu_j(z_j - z_{j+1})$  and dissipative fluxes  $\Delta_j z_j$ . In the absence of dissipation, namely, if  $\Delta_j = 0$  for all  $j$ , the equilibrium solution  $\beta_1 = \dots = \beta_M = \beta_{\text{ext}}$  is recovered. To study the dissipative case, we need to choose a specific form of the frequency  $\nu_j$  and the dissipation rate  $\Delta_j$ . A generic form is the following:

$$\nu_j = \nu_1 k_j^\alpha, \quad \Delta_j = D k_j^\gamma, \quad \gamma > 0, \quad (6)$$

where we have introduced a pseudo wave number  $k_j = m^{j-1}$ , to map the tree structure onto physical space. Parameters  $\nu_1$  and  $D$  are, respectively, a frequency characterizing the large scale dynamics, and a dissipation coefficient. We impose the condition  $\alpha < \gamma$ , so that dissipation becomes the dominant effect at small scales (large  $k_j$ ). The transfer rate  $\nu_j$  and the dissipation rate  $\Delta_j$  are balanced for a wave number  $k_j = K$  given by

$$K = \left( \frac{\nu_1}{D} \right)^{1/(\gamma-\alpha)}, \quad (7)$$

which goes to infinity in the limit of small dissipation coefficient  $D$  ( $\nu_1/D$  is similar to the Reynolds number in hydrodynamics). For large  $K$ , we shall call the ranges  $k_j \ll K$  and  $k_j \gg K$  the inertial and dissipative ranges, respec-

tively. The solution of Eqs. (3)–(5), can be evaluated numerically. We are interested in the inertial range behavior, where energy transfer dominates over dissipative effects, so that we shall explore the solutions by varying  $\alpha$  while keeping  $\gamma$  fixed. We first compute the mean energy flux  $\Phi$  injected by the reservoir,

$$\Phi = \nu_{\text{ext}}(e^{-\beta_{\text{ext}} \varepsilon_0} - e^{-\beta_1 \varepsilon_0}). \quad (8)$$

The flux  $\Phi$  is plotted as a function of  $\alpha$  in Fig. 2(a), for a broad range of values of the dissipation coefficient  $D$ . We observe a transition around the value  $\alpha = -1$ : for  $\alpha < -1$ ,  $\Phi \rightarrow 0$  when  $D \rightarrow 0$ , while for  $\alpha > -1$ ,  $\Phi$  converges to a finite value in the small  $D$  limit. These two regimes are also clearly seen in Figs. 2(b)–2(d) by plotting the temperature  $T_j = \beta_j^{-1} = -\varepsilon_0 / \ln z_j$  as a function of  $\ln k_j = (j-1) \ln m$ . A first trivial observation is that  $K$

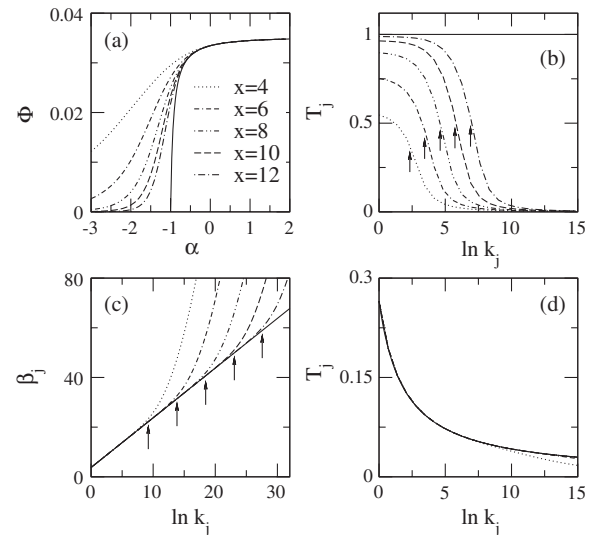


FIG. 2. Numerical solution of Eqs. (3)–(5), for  $\gamma = 2$  and  $D = 10^{-x}$ , with  $x$  given in (a); same symbols for all four figures. (a) Energy flux  $\Phi$  as a function of  $\alpha$ ; the full line is  $\Phi_0$  given in Eq. (10). (b) Temperature  $T_j = \beta_j^{-1}$  versus  $\ln k_j$  for  $\alpha = -2$ ; the full line is  $T_{\text{ext}}$ . (c)  $\beta_j$  versus  $\ln k_j$  for  $\alpha = 1$ ; full line:  $\beta_j^{\text{neq}}$  defined in Eq. (14). (d) Same data as (c) plotted as  $T_j$ , on the same window of  $\ln k_j$  as (b). Arrows in (b) and (c) indicate the value of  $K$  for each  $D$ . Other parameters:  $M = 50$ ,  $m = 2$ ,  $\nu_1 = 1$ ,  $\nu_{\text{ext}} = 0.1$ ,  $\beta_{\text{ext}} = 1$ ,  $\varepsilon_0 = 1$ .

increases more rapidly when decreasing  $D$  for larger values of  $\alpha$ . More interestingly, we observe that for  $\alpha = -2$  [Fig. 2(b)], the temperature profile slowly converges to the equilibrium profile  $T_j^{\text{eq}} = \beta_{\text{ext}}^{-1}$  when  $D \rightarrow 0$ , while for  $\alpha = 1$  [Figs. 2(c) and 2(d)], it converges to a well-defined nonequilibrium profile, which is linear for  $k_j \lesssim K$  when plotting  $\beta_j$  as a function of  $\ln k_j$  [see Fig. 2(c)]. These results can be interpreted as follows. When the transfer mechanism is inefficient at small scales ( $\alpha < -1$ ), dissipative scales are not “fed,” so that energy accumulates at large scales, generating an effective equilibrium. In the opposite case ( $\alpha > -1$ ), the transfer mechanism is efficient at small scales, thus “pumping” energy from large scales to dissipative ones.

Most of the above behavior can be understood using a simpler form of the dissipation, which leads to analytically tractable calculations. We assume that  $\Delta_j = 0$  for all  $j < M$ , leaving a nonzero dissipation rate  $\Delta_M$  only on the last level  $j = M$  of the tree. As a first step, we look for the solutions of Eqs. (3) and (4) with  $\Delta_j = 0$ ,  $j = 1, \dots, M - 1$ , without taking into account the dissipative boundary condition (5). For  $\alpha \neq -1$ , we find a family of solutions, parametrized by the flux  $\Phi$ :

$$z_j = e^{-\beta_{\text{ext}}\varepsilon_0} \left[ 1 - \Phi \left( \frac{1}{\Phi_0} - \frac{1}{Bk_j^{1+\alpha}} \right) \right], \quad (9)$$

where  $j = 1, \dots, M$ , and with  $\Phi_0$  and  $B$  given by

$$\Phi_0 = \frac{\nu_1(m - m^{-\alpha})\nu_{\text{ext}}e^{-\beta_{\text{ext}}\varepsilon_0}}{\nu_1(m - m^{-\alpha}) + \nu_{\text{ext}}}, \quad (10)$$

$$B = \nu_1(m - m^{-\alpha})e^{-\beta_{\text{ext}}\varepsilon_0}. \quad (11)$$

Note that  $z_j$  smoothly converges to  $e^{-\beta_{\text{ext}}\varepsilon_0}$  when  $\Phi \rightarrow 0$ , and is a decreasing function of  $k_j$  for  $\Phi > 0$ . Interestingly, Eq. (9) imposes an upper bound  $\Phi_{\text{max}}$  on the flux  $\Phi$ , which is determined by the condition  $z_M > 0$ :

$$\Phi_{\text{max}} = \left( \frac{1}{\Phi_0} - \frac{1}{Bk_M^{1+\alpha}} \right)^{-1}. \quad (12)$$

If  $\alpha < -1$ , one finds for large  $M$  that  $\Phi_{\text{max}} \approx |B|k_M^{-|1+\alpha|}$ , so that  $\Phi_{\text{max}} \rightarrow 0$  when  $M \rightarrow \infty$ . Accordingly, whatever the small scale boundary condition, the flux vanishes in the large size limit. In contrast, if  $\alpha > -1$ ,  $\Phi_{\text{max}}$  converges to  $\Phi_0 > 0$  in the large size limit  $M \rightarrow \infty$ ;  $\Phi_0$  goes to zero linearly with  $\alpha$  when  $\alpha \rightarrow -1^+$ .

We now use the dissipative boundary condition (5) to determine the precise value of the flux. Equation (5) states that the diffusive flux  $\Phi$  is equal to the dissipated flux on level  $j = M$ . This condition leads to  $\Phi = m^{M-1}\Delta_M z_M$ , or using  $k_M = m^{M-1}$ ,  $z_M = \Phi/(k_M\Delta_M)$ . Equating this value of  $z_M$  with that given in Eq. (9) for  $j = M$ , yields an equation for  $\Phi$ , which is solved into

$$\Phi = \Phi_{\text{max}} \left( 1 + \frac{e^{\beta_{\text{ext}}\varepsilon_0}\Phi_{\text{max}}}{k_M\Delta_M} \right)^{-1}. \quad (13)$$

Identifying  $k_M$  with the value  $K$  defined in Eq. (7), we get

$\Delta_M = DK^\gamma = \nu_1 K^\alpha$ , and thus  $k_M\Delta_M = \nu_1 K^{1+\alpha}$ . For  $\alpha < -1$ , both  $k_M\Delta_M$  and  $\Phi_{\text{max}}$  are for large  $K$  proportional to  $K^{-|1+\alpha|}$ , so that their ratio is a constant. From Eq. (13),  $\Phi$  goes to zero as a finite fraction of the maximum flux  $\Phi_{\text{max}}$ . Using  $K \sim D^{-1/(\gamma-\alpha)}$ , the flux  $\Phi$  behaves in terms of the dissipation coefficient as  $\Phi \sim D^\mu$  when  $D \rightarrow 0$ , with  $\mu = |1+\alpha|/(\gamma-\alpha)$ . From Eq. (9),  $\beta_j \rightarrow \beta_{\text{ext}}$  when  $D \rightarrow 0$ , as long as  $k_j \ll K$ . Altogether, the effect of dissipation on the system may be considered as perturbative in the case  $\alpha < -1$ . The perturbation expansion is, however, singular, with a nontrivial exponent  $\mu < 1$ . In the opposite case  $\alpha > -1$ ,  $\Phi_{\text{max}} \rightarrow \Phi_0 > 0$ , while  $k_M\Delta_M \rightarrow \infty$ . Hence from Eq. (13),  $\Phi$  is equal for large  $K$  (or small  $D$ ) to the maximum flux  $\Phi_{\text{max}} = \Phi_0$ , consistently with Fig. 2(a) [12]. From Eq. (9), the temperature profile  $\beta_j = -\varepsilon_0^{-1} \ln z_j$  converges to a well-defined nonequilibrium profile

$$\beta_j^{\text{neq}} = \frac{1}{\varepsilon_0} (1 + \alpha) \ln k_j + \beta_{\text{ext}} + \frac{1}{\varepsilon_0} \ln C, \quad (14)$$

with  $C = 1 + \nu_1(m - m^{-\alpha})/\nu_{\text{ext}}$ . Although this profile has been obtained with a simplified version of the model, one sees on Fig. 2(c) that  $\beta_j$  computed numerically in the original model also converges to  $\beta_j^{\text{neq}}$ . Let us emphasize that  $\beta_j^{\text{neq}}$  does not depend on parameters related to dissipation [13], but only on parameters characterizing injection and transfer. The temperature profile is continuous with  $\alpha$ , namely  $\beta_j \rightarrow \beta_{\text{ext}}$  when  $\alpha \rightarrow -1^+$ . Note also that the coupling  $\nu_{\text{ext}}$  simply renormalizes the inverse temperature  $\beta_{\text{ext}}$ ; the low coupling limit corresponds to driving the system with a small effective temperature.

To sum up, it turns out that an equilibrium approach to the stationary state of the present model in the weak dissipation limit is meaningful only if  $\alpha < -1$ . In this case, the probability distribution  $P_{\text{st}}(\{n_{j,i}\})$  converges, in a weak sense, to the equilibrium distribution of temperature  $\beta_{\text{ext}}$ . In the opposite case  $\alpha > -1$ , the probability distribution  $P_{\text{st}}(\{n_{j,i}\})$  converges when  $D \rightarrow 0$  to a well-defined nonequilibrium probability distribution  $P_{\text{neq}}(\{n_{j,i}\})$ , given by Eqs. (2) and (14) [14]. In order to discuss the implications of such different behaviors, we now compute the average value of large scale observables, which are not sensitive to small scale details of the distribution and in principle accessible to measurements in real systems. These include observables  $Y$  defined as

$$Y = \sum_{j=1}^M \left( g(k_j) \sum_{i=1}^{m^{j-1}} f(n_{j,i}) \right), \quad (15)$$

where  $f(n)$  is an arbitrary function, and  $g(k)$  satisfies  $kg(k) \rightarrow 0$  when  $k \rightarrow \infty$ . Figure 3(a) illustrates the convergence of  $\langle Y \rangle$  as a function of  $\alpha$ . When  $\alpha < -1$ ,  $\langle Y \rangle$  converges to the equilibrium value  $\langle Y \rangle_{\text{eq}}$ . In contrast, for  $\alpha > -1$ ,  $\langle Y \rangle$  converges to the nonequilibrium value  $\langle Y \rangle_{\text{neq}}$  (computed from the distribution  $P_{\text{neq}}$ ), which depends on  $\alpha$  and thus on the energy transfer.

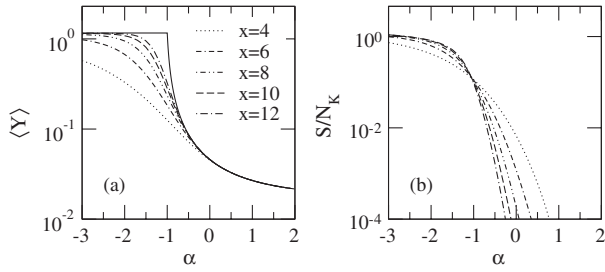


FIG. 3. (a)  $\langle Y \rangle$  as a function of  $\alpha$ , for  $D = 10^{-x}$ ;  $Y$  is defined in Eq. (15), with here  $f(n) = n$  and  $g(k) = k^{-2}$ . The full line is the asymptotic value of  $\langle Y \rangle$  for  $D \rightarrow 0$ . (b) Normalized entropy  $S/N_K$  versus  $\alpha$ , for the same values of  $D$  as (a). Other parameters: same as in Fig. 2.

Other relevant statistical quantities are sensitive to the small scale details of the distribution, and have a more complex behavior. This is the case of the entropy  $S = -\sum_{\{n_{j,i}\}} P_{\text{st}}(\{n_{j,i}\}) \ln P_{\text{st}}(\{n_{j,i}\})$ . Figure 3(b) shows the normalized entropy  $S/N_K$ , where  $N_K = mK/(m-1)$  is the volume of the inertial range (i.e., the number of sites with  $k_j \leq K$ ). Convergence to a limit curve is observed only for  $\alpha < -1$ . From a simple scaling argument, we find that  $S$  is proportional to  $N_K$  if  $\alpha < -1$  and to  $N_K^{|\alpha|}$  if  $-1 < \alpha < 0$ , while  $S$  is independent of  $N_K$  for  $\alpha > 0$ . Hence the dissipative state characterized by  $P_{\text{neq}}(\{n_{j,i}\})$  has a much lower entropy than the quasiequilibrium state obtained for  $\alpha < -1$  and the accessible volume in phase space is much smaller than in equilibrium states.

Finally, we consider the energy spectrum, a quantity often reported in experiments. For dissipative systems described by hydrodynamic equations, energy transfer between modes is most often due to the nonlinear terms in these equations (instead of the linear diffusive dynamics of the present model). Assuming the dominant nonlinear term to be of order  $p$ , and to involve  $q$  space derivatives (e.g.,  $p = 2$  and  $q = 1$  for the Navier-Stokes equation), a generalization of Kolmogorov K41 argument [2] leads to an energy spectrum proportional to  $\Phi_0^\mu k^{-\eta}$  with  $\mu = 2/(p+1)$  and  $\eta = 1 + q\mu$ , where  $\Phi_0$  is the dissipated energy flux. This dimensional argument implicitly assumes that the dissipated flux remains finite in the low dissipation limit. In the present model, the energy spectrum is  $\langle n_{i,j} \varepsilon_0 \rangle \propto \Phi_0 k_j^{-1-\alpha}$ ; by identification, we get  $p = 1$  (in agreement with the diffusive dynamics of the model) and, more interestingly,  $\alpha = q$ . Hence the parameter  $\alpha$  may be interpreted as the order of derivation in the hydrodynamic transfer term. Note that we thus expect  $\alpha \geq 0$ , consistently with the assumption of a finite dissipated flux. It would be interesting to generalize the model to account for the case  $p > 1$  (where nontrivial scalings of the spectrum with  $\Phi_0$  appear) and for other types of geometries, such as finite-dimensional lattices [15].

The major interest of our model is to provide the exact solution for the nonequilibrium probability distribution of microscopic configurations, thus giving insights on how to

build a statistical physics for dissipative systems. Indeed, our results suggest a simple approximation scheme to describe the far-from-equilibrium state of weakly dissipative systems, by assuming (i) that each scale is equilibrated at a given temperature, and decorrelated from the others, and (ii) that the dissipated flux is the maximal one given the injection mechanism. Although very simple, this strategy yields exact results in the present model, and may be considered as a mean-field treatment in more general situations. Testing the predictions of this approach in realistic models would be of great interest.

- [1] R. Kubo, M. Toda, and N. Hashitsume, *Statistical Physics* (Springer, New York, 1995), Tome 2.
- [2] U. Frisch, *Turbulence* (Cambridge University Press, Cambridge, 1995).
- [3] V.E. Zakharov, V.S. Lvov, and G. Falkovich, *Kolmogorov Spectra of Turbulence I: Wave Turbulence* (Springer-Verlag, Berlin, 1992).
- [4] G. Düring, C. Josseland, and S. Rica, Phys. Rev. Lett. **97**, 025503 (2006); A. Boudaoud, O. Cadot, B. Odille, and C. Touzé, Phys. Rev. Lett. **100**, 234504 (2008).
- [5] M. J. Alava, P. K. V. V. Nukala, and S. Zapperi, Adv. Phys. **55**, 349 (2006); E. Bouchbinder, I. Procaccia, and S. Sela, J. Stat. Phys. **125**, 1025 (2006).
- [6] A. Volmer and T. Nattermann, Z. Phys. B **104**, 363 (1997).
- [7] P. K. Haff, J. Fluid Mech. **134**, 401 (1983); H. M. Jaeger, S. R. Nagel, and R. P. Behringer, Rev. Mod. Phys. **68**, 1259 (1996); M. Lundberg, K. Krishan, N. Xu, C. S. O'Hern, and M. Dennin, Phys. Rev. E **77**, 041505 (2008).
- [8] D. Montgomery and G. Joyce, Phys. Fluids **17**, 1139 (1974); J. Miller, Phys. Rev. Lett. **65**, 2137 (1990); R. Robert, J. Stat. Phys. **65**, 531 (1991); R. Robert and J. Sommeria, J. Fluid Mech. **229**, 291 (1991); P. H. Chavanis, Phys. Rev. Lett. **84**, 5512 (2000); N. Leprovost, B. Dubrulle, and P. H. Chavanis, Phys. Rev. E **73**, 046308 (2006).
- [9] S. Aumaître, S. Fauve, S. McNamara, and P. Poggi, Eur. Phys. J. B **19**, 449 (2001).
- [10] E. Levine, D. Mukamel, and G. M. Schütz, J. Stat. Phys. **120**, 759 (2005); R. J. Harris, A. Rákos, and G. M. Schütz, J. Stat. Mech. (2005) P08003; J. D. Noh, Phys. Rev. E **72**, 056123 (2005); M. R. Evans and T. Hanney, J. Phys. A **38**, R195 (2005).
- [11] D. Stauffer and A. Aharony, *Introduction to Percolation Theory* (Taylor and Francis, London, 1998).
- [12] Similar results are obtained if one chooses a constant value  $\Delta_M = \Delta_0$  instead of  $\Delta_M = \nu_1 K^\alpha$ .
- [13] Obviously,  $\beta_j^{\text{neq}}$  cannot depend on  $D$  as the limit  $D \rightarrow 0$  is taken, but it could depend on  $\gamma$ .
- [14] The zero dissipation limit should, however, be taken after the infinite size limit; otherwise, equilibrium is recovered.
- [15] A direct extension of our definitions to a one-dimensional lattice ( $m = 1$ ) leads to constant transfer frequencies  $\nu_j$ , so that, up to the dissipation rates, one should essentially recover the standard one-dimensional open ZRP. Modifying the definition of  $\nu_j$ , one could include a  $j$  dependence even in one dimension and recover results qualitatively analogous to the ones obtained on the tree.